Magnetic Analysis of Supersonic Beams of Atomic Oxygen, Nitrogen, and Chlorine Generated from a Radio-Frequency Discharge

ARTICLE *in* ISRAEL JOURNAL OF CHEMISTRY · JANUARY 1997

Impact Factor: 2.22 · DOI: 10.1002/ijch.199700038

10 AUTHORS, INCLUDING:

Michele Alagia
Italian National Research Council
146 PUBLICATIONS **2,009** CITATIONS
SEE PROFILE

Daniela Ascenzi
Università degli Studi di Trento
76 PUBLICATIONS **1,387** CITATIONS
SEE PROFILE

Nadia Balucani
Università degli Studi di Perugia
162 PUBLICATIONS **3,467** CITATIONS
SEE PROFILE

David Cappelletti
Università degli Studi di Perugia
151 PUBLICATIONS **3,325** CITATIONS
SEE PROFILE

Magnetic Analysis of Supersonic Beams of Atomic Oxygen, Nitrogen, and Chlorine Generated from a Radio-Frequency Discharge

MICHELE ALAGIA,[a,*] VINCENZO AQUILANTI,[a] DANIELA ASCENZI,[a] NADIA BALUCANI,[a] DAVID CAPPELLETTI,[b] LAURA CARTECHINI,[a] PIERGIORGIO CASAVECCHIA,[a] FERNANDO PIRANI,[a] GIAMPAOLO SANCHINI,[a] AND GIAN G. VOLPI[a]

[a]Dipartimento di Chimica, Università di Perugia, Via Elce di Sotto 8, Perugia 06123, Italy

[b]Istituto per le Tecnologie Chimiche, Università di Perugia, Perugia 06125, Italy

(Received 10 July 1997 and in revised form 5 August 1997)

Abstract. Supersonic beams of oxygen, nitrogen, and chlorine atoms and of metastable oxygen and nitrogen molecules produced from a high-pressure radio-frequency discharge beam source have been characterized by coupling velocity selection with magnetic analysis in the transmission mode. The present work leads to the determination of the relative populations of the electronic states of the species in the produced beams, showing that estimates of the populations from plasma temperatures or final translational temperatures could bring on incorrect conclusions.

INTRODUCTION

Elastic, inelastic, and reactive collisions of open shell species play a dominant role in many chemical processes from combustion to plasma chemistry, from atmospheric to interstellar chemistry. The study of the detailed dynamics of such processes requires intense and state-selected beams. Continuous intense beams of open shell atoms and free radicals can be efficiently produced from dissociation of stable molecules in plasma excited in electrical discharge cavities, and their internal quantum state distribution can be characterized by Stern–Gerlach magnetic analysis.

Magnetic analysis of atomic beams generated by microwave (MW) discharges has long been used in this laboratory[1] to control the population of fine structure levels for elastic scattering experiments aimed at studying interactions of open shell species. The characteristics of such beams—effusive or nearly supersonic, broad thermal velocity distributions—are not well suited for reactive scattering experiments, where higher intensities and narrower velocity spreads are desirable.

Sibener et al.,[2] drawing on the work of Miller and Patch,[3] developed a radio-frequency (RF) discharge source for the production of supersonic beams of oxygen atoms, which could operate at higher pressures and plasma temperatures than a MW discharge,[4] giving a much higher degree of molecular dissociation, and hence permitting the production of beams with a lower velocity spread and the achievement of higher fluxes and translational energies. The study of Sibener et al. showed that when dilute mixtures of O_2 in He were used, some electronically excited states of atomic oxygen were also produced,[2,5] in particular $O(^1D)$, a metastable species with a lifetime of 150 s, whose chemical behavior is of extreme importance in atmospheric chemistry.

In our laboratory we developed a RF discharge source which was optimized for the production of $O(^1D)$; the aim was to investigate the reaction dynamics of $O(^3P)$ and/or $O(^1D)$ with simple molecules in crossed beam experiments.[6–11] More recently, by exploiting the versatility of the RF discharge source, the method has been successfully applied to generate intense continuous beams of $OH(^2\Pi)$ radicals, $Cl(^2P)$, and $N(^4S, ^2D, ^2P)$ atoms, allowing us to study the reaction dynamics of these species with simple molecules.[8,9,12–15] Although this was the first time, to our knowledge, that a RF discharge was used to generate OH radical and atomic Cl beams, we recall that a MW discharge beam source of effusive OH and supersonic Cl was successfully used in crossed molecular beam experiments by Grice and coworkers.[4] However, in these cases, the RF discharge method gives higher beam intensities and speed ratios than the MW discharge method, as already noted for oxygen atom beams. Intense continuous chlorine atom beams were also produced in a resistively heated high density graphite nozzle by Valentini et al.[16] and used in crossed beam experiments.[16,17] On the contrary, the difficulty of generating N atom beams of sufficient inten-

*Author to whom correspondence should be addressed. E-mail: mik@scatter.chm.unipg.it.

sity limited collisional studies of this important species, despite its fundamental role in such areas as astrochemistry, combustion, and atmospheric chemistry. Bernstein and coworkers produced intense beams of N atoms in a Knuth-type arc-heated Ar nozzle source;[18,19] Ringer and Gentry generated atomic N beams by neutralizing the N^+ ionic beam produced by 75 eV electron bombardment of N_2 [20] through charge exchange with Ar. Porter et al.[21] formed N atom beams from the exit slit of a condensed dc discharge through flowing N_2 at about 1 mbar. A more recent source was developed by Pollard:[22] supersonic beams of atomic nitrogen and oxygen were produced by a RF discharge within a ceramic nozzle; high flux of atoms are obtained by using mixtures of N_2 seeded in He at a stagnation pressure of 260–330 mbar. However, no reactive scattering studies of N atom reactions were reported in which angular and velocity distributions of the products were measured. The supersonic beams of N atoms generated by the present RF discharge source were the first of sufficient intensity to be used for reactive scattering studies of N atom reactions, where product angular and velocity distributions were measured.[14,15]

Since a manifold of electronic and fine structure levels are usually populated when electric discharge plasma are used, the internal state analysis and control are basic problems; atoms and radicals can undergo a substantial relaxation to low-lying quantum states when supersonic conditions are used: the relaxation occurs during the nozzle expansion because of the high number of collisions among particles. Reaction dynamics may be affected by the quantum states of colliding partners and, therefore, a state characterization of the beams is desirable. Non-optical methods, which exploit suitable external electric or magnetic fields, represent powerful means for state analysis and selection of atomic and molecular beams.[23] The Stern–Gerlach magnetic selector in Rabi configuration, employed in the present experiments, makes use of an inhomogeneous field which operates between the convex and concave surfaces of different radii of two iron poles. The action of such a field on a velocity-selected beam of a paramagnetic species induces selective deflection depending on the value of the effective magnetic moment, i.e., the component of the magnetic moment along the field gradient direction, which is defined in terms of the Zeeman energy of each quantum state. In the past, magnetic selection techniques were used in some direct applications to physicochemical problems,[24–33] to measure anisotropic effects in collisions of open shell atoms with rare gases,[34–38] and to state analyze reagents and products in reactive processes.[39–41]

In our configuration the detector measures on line the beam transmittance across the magnet, defined as the ratio between the beam intensity with and without the applied field. The beam transmittance decreases as a function of the magnetic field intensity, with values and slopes which depend on weight and type of the sublevels actually deflected at that field strength. In this way, it is possible to control and to vary the sublevel distribution in the beam transmitted to the detector.

In the past, we applied magnetic analysis in the transmission mode to characterize the sublevel distributions of open shell atoms (N,[42] O,[43] F,[44] and Cl[45]) in effusive or moderately supersonic beams produced from MW discharge sources operating at low pressure (in the mbar range), and to perform integral cross section measurements under controlled conditions of atomic sublevels.[46] The same method was also applied for the diagnostics of molecular beams containing N_2 [47] and O_2 [48] molecules both in the ground and in metastable states, leading to an estimate of the mean collision-free lifetime of the $^5\Sigma_g^+$ metastable state of nitrogen molecules, one of the electronic states which can be relevantly populated in a discharge-generated plasma,[47] and to the characterization of collisional alignment effects in seeded supersonic beams of molecular oxygen.[49]

The present work deals with the diagnostic of the above-mentioned supersonic beams of open shell atoms (Cl, O, and N) produced by the RF discharge and extensively used in crossed beam experiments.

EXPERIMENTAL

A simplified scheme of the experimental apparatus, consisting of a set of differentially pumped chambers connected by various holes and skimmers for the collimation of the beam, is displayed in Fig. 1.

A sectioned side view of our RF discharge beam source is shown in Fig. 2. It consists of a parallel LC circuit made to resonate around 14 MHz which feeds high levels of RF power into a plasma contained in a quartz nozzle, cooled with low electrical conductivity water. The design is similar to that described by Sibener et al.[2] The water cooling jacket surrounding the final part of the quartz nozzle is needed to prevent the orifice from melting and/or enlarging during the expansion of the hot gas plasma; the geometry of the nozzle tip was designed to have the water cooling flow as close as possible to the orifice (due to the poor thermal conductivity of quartz). Water cooling also gives the advantage of reducing the atomic recombination on the quartz nozzle walls. Low electrical conductivity water is used as a nozzle coolant, since regular water caused significant RF power loss. Nozzle diameters are typically 0.20–0.26 mm. The tube containing the gas to be discharged is centered about the tank coil (L) of a variable frequency oscillator; the coil is differentially wound around the front of the nozzle and is water cooled as well. To prevent drawbacks, due to the circuit loading changes when the gas pressure reaches several hundred millibars, the oscillator is

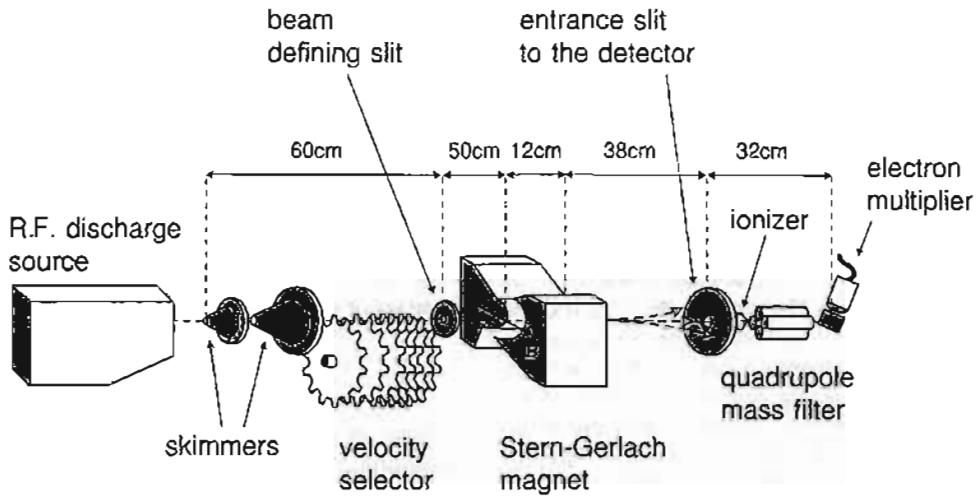

Fig. 1. A simplified scheme of the experimental apparatus.

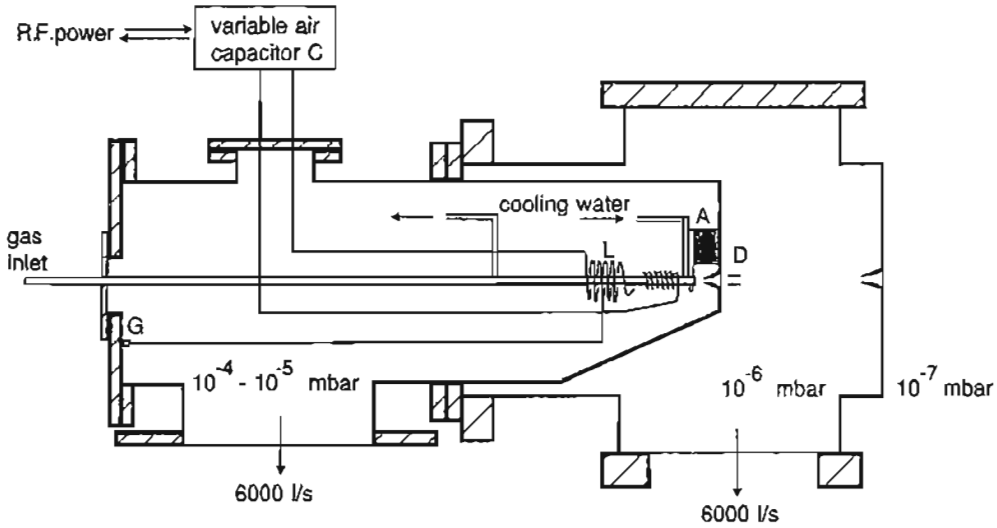

Fig. 2. Sectioned side view of the radio-frequency discharge beam source mounted in a differentially pumped chamber of the apparatus.

separated from the load by a stage of amplification. This arrangement also allows a good match of the impedance of the discharge with that of RF electronics. The RF power is supplied by a solid state, home built radio transmitter which can deliver a maximum output of 100 W over a frequency range centered at about 14 MHz; the transmitter is followed by a linear amplifier capable of providing RF output levels above 500 W. A variable home built air capacitor (C) is placed outside the source chamber in order to easily achieve the frequency matching of the internal circuit to the electronics when the source is operating under vacuum. Crucial for the discharge operation is the presence and the position of a variable ground tap (G) on the tank coil, whose function is to produce a large step-down of the plasma impedance, made possible by the coupling coil-tap system working as a RF autotransformer. The impedance transformation depends on the square of the ratio between the total number of coil turns and the number of turns from the rear of the coil to the ground tap and generates a large voltage step-up at the front of the coil, i.e., near the nozzle tip. The position of the ground tap was fixed by testing the discharge performance (typically SWR did not exceed 1.25:1), and in many cases the coupling was good enough so that additional fine tuning through an impedance matching circuit was not required. The tuning of

the circuit is monitored by an in-line RF wattmeter with a standing wave ratio bridge. A very important characteristic of the beam source is the plasma localization directly behind the orifice of the nozzle, permitting very high degrees of dissociation (indeed, without the plasma localization at the nozzle tip, atomic recombination would be extensive) obtained by placing an electrically grounded block of aluminum (A) around the nozzle tip. At relatively high pressure a coupling between the front tank coil turns and the grounded aluminum block is achieved, making the discharge capacitively coupled and no longer inductively coupled. The stronger the coupling, the more the plasma is localized towards the front of the nozzle. The skimmers (typical openings ~1 mm) are made of boron nitride, an electrical insulating material easy to machine, which did not degrade after many months of discharge working. Some ions are formed in the hot plasma and pass through the nozzle skimmer; they are deflected out of the beam by an electrical field (D) located in front of the collimating slit in the differential pumping region.

A severe limitation for this beam source is the pumping system efficiency. In our configuration the source chamber is pumped by a 6000 liter/s diffusion pump backed by a 500 m^3/h root pump and a 35 m^3/h rotary pump. The large pumping speed is necessary in order to keep the background source pressure below 1×10^{-4} mbar; at higher background pressure the RF power decouples and a glow discharge occurs.

The beam, in a collision-free flight through an intermediate collimation chamber and a defining hole, proceeds to a chamber (background pressure ~10^{-7} mbar) which contains a mechanical velocity selector and a magnetic analyzer. The velocity selector consists of eight rapidly spinning, slotted disks which transmit a fraction of the beam (fwhm ~5%) into the region where magnetic deflection takes place. The magnetic analyzer is a Stern–Gerlach magnet in the Rabi configuration working in the transmission mode having the following dimensions and technical features: length ℓ ~12 cm, curvature radius of the convex pole ~0.35 cm, gap between the two pole faces ~0.4 cm with the beam traveling approximately halfway in the magnet gap. For this "two wire"-like configuration the field gradient is proportional to the field itself: empirically we find $\partial B/\partial z \cong 3.0B$, where the proportionality factor 3.0 is in units of cm^{-1}.

To detect particles emerging from the magnet, use is made of an electron impact quadrupole mass spectrometer contained in an ultra-high-vacuum (10^{-10} mbar) chamber. The detector chamber is connected to the apparatus by an intermediate chamber, which is necessary to place the detector at a sufficiently large distance from the magnetic analyzer in order to obtain a high angular resolution in the deflection experiments.

BEAM DIAGNOSTICS

The open-shell atomic and molecular beams have been characterized by measuring their velocity distributions and magnetic transmittances. The velocity and magnetic analysis give information on the translational and internal state distributions, respectively.

When a paramagnetic particle travels at a selected velocity v, inside an inhomogeneous magnetic field whose gradient in the direction z perpendicular to the particle motion is $\partial B/\partial z$, it undergoes a deflection along the z direction. This deflection d, at a distance $\mathcal{L}$ (=38 cm in our case) from the magnet exit slit to the detector slit, depends on the mass m and speed v of the particle, on the length ℓ of the magnet, and on the effective magnetic moment μ_i of the molecule or atom, where i is an appropriate set of quantum numbers:

$$d = \ell\left(\frac{\ell}{2} + \mathcal{L}\right)\frac{\mu_i}{mv^2}\frac{\partial B}{\partial z} \qquad (1)$$

Since in our case $\partial B/\partial z \cong 3.0B$, the deflection is proportional to B. This formula follows from elementary kinematic considerations, once it is taken into account that the particle motion along the direction orthogonal to the initial motion can be considered as uniformly accelerated within the magnet for a length ℓ and uniformly rectilinear outside the magnet for a length $\mathcal{L}$.

The relevant measurable parameter in our experiment is the beam transmittance I/I_0, i.e., the ratio between the beam intensity with and without the applied field. The transmittance is a decreasing function of the magnetic field strength: since it is possible to correlate the rate of decrease with the effective magnetic moments of the particles deflected from the molecular beam direction, the measurement of the beam transmittance at selected velocities v allows us to characterize the beam composition and internal states distribution.

The working equation for beam transmittance is as follows:

$$\frac{I}{I_0} = \sum_i W_i \mathcal{T}(B, v, \mu_i) \qquad (2)$$

where W_i are the relative weights of the magnetic sublevels in the original beam (i.e., with no field applied) and $\mathcal{T}$—an empirically determined instrumental function ranging between 0 and 1—represents the transmission factor of each molecular sublevel: it depends on the beam size, on the geometric factors of the apparatus and on the selective deflection of the particles in the sublevels i.

The value of the beam transmittance across the Stern–Gerlach magnetic selector at a given magnetic field intensity is the result of the extent by which each sublevel is deflected (see eq 1) in comparison with the dimension of the detector slit—those sublevels showing a deflection higher than the detector slit dimension being responsible for the decrease in the beam transmittance. As can be seen from eq 1, the deflection of each sublevel can be obtained once the effective magnetic

moment has been calculated. In a definite angular momentum-coupling scheme in the magnet, giving J as the resulting vector, the "good" quantum numbers are labeled as J and M_J; the latter defines the projection of J along the z direction. The ket $|J\ M_J\rangle$ properly describes the particle state i in the field, and the effective magnetic moment is:

$$\mu_{JMJ} = \mu_0\, g_J\, M_J \tag{3}$$

where $\mu_0 = 9.27 \cdot 10^{-28}$ J/Gauss is the Bohr magneton, and g_J is the Landé g-factor relative to the quantum number J.

The more frequent situation in the magnet corresponds to a partial decoupling of angular momenta, therefore it is necessary to calculate the effective magnetic moment from its general definition which, for a particle in a quantum state i having a potential energy E_i in an external magnetic field, is:[50]

$$\mu_i = -\frac{\partial E_i}{\partial B} \tag{4}$$

RESULTS AND DISCUSSION

Supersonic beams of oxygen, nitrogen, and chlorine atoms were produced from the RF discharge beam source starting from different mixtures of O_2, N_2, and Cl_2 in Ne or He, as seeding gases. Experimental conditions used for beams production are summarized in Table 1, which lists the source stagnation pressure P_0, the RF discharge nominal power p, and the plasma temperature T_0. The table also reports the main features of the beams, such as peak velocities v_{peak}, Mach numbers M_f, and final translational temperatures T_f, obtained from the best fit of the measured velocity distributions, by using the appropriate formulas for seeded supersonic beams.[51]

The plasma temperature T_0 may be estimated from the variation of the flux Φ of the gas coming from the nozzle. In fact, the flux is proportional to the product of the particle number density $n(T)$ and the velocity of the beam particles $v(T)$, which depend on T^{-1} and $\sqrt{T}$, respectively, and therefore

$$\Phi(T) \propto n(T) \cdot v(T) \propto 1/\sqrt{T} \tag{5}$$

Since the flux is proportional to the source pressure, an estimate of T_0 can be made by measuring pressure variations with the discharge on and off:

$$\frac{P_{on}}{P_{off}} = \frac{\Phi_{on}}{\Phi_{off}} = \sqrt{\frac{T_{off}}{T_{on}}} \tag{6}$$

where T_{off} is assumed to be 300 K and $T_0 = T_{on}$.

The plasma temperature, T_0, shows a dependence on stagnation pressure and discharge power. In general, a decrease of pressure or an increase of power produces a rise of T_0 due to the reduced gas flux at the orifice. The nature of the seeding gas has a strong influence on the performance of the discharge and on T_0: the larger the mass of the seeding gas, the higher the T_0.

The extent of molecular dissociation in the beam was estimated for all the O_2/He (or Ne), N_2/He (or Ne), and Cl_2/He (or Ne) mixtures as a function of gas pressure and RF power. The relative number densities N of atomic and molecular species (hereafter X and X_2) in the beam were measured by integrating the time-of-flight spectra of the masses corresponding to both X and X_2 in order to eliminate spurious interferences. To correctly evaluate the degree of molecular dissociation α, since some of the signal registered at the X mass may be generated by dissociative ionization of the X_2 molecule in the ionizing region, the dissociative ionization cross section σ_{d_i} relative to the process

$$X_2 \xrightarrow{+e^-} X + X^+ + 2e^- \tag{7}$$

has to be known. According to the expression derived

Table 1. Main features of atomic supersonic beams produced in the present experiment

	Seeding gas	P_0 (mbar)[a]	p (Watt)[b]	T_0 (K)[c]	v_{peak} (m·s^{-1})[d]	M_f[e]	T_f (K)[f]	α[g]
O atom beams								
	Ne	120 ± 2	310	1500 ± 200	1390 ± 30	7.6 ± 0.8	100 ± 10	0.90
	He	127 ± 2	275	1200 ± 200	2500 ± 50	9.0 ± 1.0	50 ± 5	0.85
N atom beams								
	Ne	267 ± 3	300	1800 ± 200	1550 ± 30	8.0 ± 0.8	90 ± 9	0.60
	He	240 ± 3	300	1700 ± 200	2980 ± 60	10.0 ± 1.0	40 ± 4	0.60
Cl atom beams								
	Ne	176 ± 2	300	1500 ± 200	1570 ± 20	8.0 ± 0.8	85 ± 8	0.95
	He	300 ± 3	300	1200 ± 200	2720 ± 50	9.0 ± 1.0	55 ± 5	0.90

[a]Stagnation source pressure. [b]RF nominal power. [c]Plasma temperature. [d]Peak velocity. [e]Mach number. [f]Translational temperature, as obtained from velocity distribution. [g]Degree of precursor molecular dissociation.

by Miller and Patch,[3] α may be estimated by

$$\alpha = \frac{R}{R+2} \tag{8}$$

where R is the number density ratio $\frac{N_X}{N_{X_2}}$ with the discharge on. R can be calculated from

$$R = \frac{N_X}{N_{X_2}} = \frac{\sigma_{X_2}/\sigma_{d.i.}}{\eta} \cdot \frac{\sigma_{X_2}}{\sigma_X} \cdot \frac{I_{X_{on}} - \eta I_{X_{2on}}}{I_{X_{2on}}} \tag{9}$$

where σ_X and σ_{X_2} are the ionization cross section, and $I_{X_{on}}$ and $I_{X_{2on}}$ are the integrated areas of the time-of-flight spectra of the atomic and molecular species, respectively; η is the ratio $\frac{I_{X_{on}}}{I_{X_{2on}}}$ with discharge off, and accounts for any possible difference in the detection efficiency for X and X_2 masses. For oxygen and nitrogen σ_{X_2}, σ_X, and $\sigma_{d.i.}$ are available in the literature,[52-57] while for Cl_2 the dissociative ionization cross-section is not known. In this case a rough estimate of the dissociative extent can be obtained by the following approximate equation:[4]

$$\alpha = 1 - \frac{I_{X_{2on}}}{I_{X_{2off}}} \tag{10}$$

The dissociation degree increases slightly with reducing stagnation pressure and/or increasing RF power, is larger for mixtures in Ne than for those in He, and is favored by a further dilution of the precursor gas. The dissociation degrees relative to the beams characterized in this work are reported in Table 1. Typical atomic fluxes are ~10^{18} atoms sr^{-1} s^{-1} for all cases.

Atomic Oxygen

Beams of oxygen atoms have been produced starting from two different mixtures of 2.5% O_2 in helium and in neon as carrier gases. O atoms produced in the RF discharge are mainly in their ground electronic state ^3P_J (J = 0, 1, and 2), but an appreciable fraction is also generated in the first excited metastable $^1D_2$ state, lying 1.97 eV above the ground state.[58] Measured velocity distributions are reported in Fig. 3 and beam transmittance measurements, performed for the analysis of beam compositions, are presented in Figs. 4 and 5.

The oxygen atom ^{16}O, having nuclear spin I = 0, shows no hyperfine structure and exhibits a coupling between orbital **L** and spin **S** angular momenta to give the total electronic angular momentum **J**. The energy splitting $\Delta_{J,J+1}$ between fine structure levels in the ^3P_J electronic state, $\Delta_{1,2}$ = 19.6 meV and $\Delta_{0,2}$ = 28.1 meV, are sufficiently high to assure that magnetic field strengths used in our apparatus (maximum reachable value ≅10 kGauss) are insufficient to decouple **J** in **L** and **S** (Paschen-Back effect), so that relevant quantum numbers are J and M_J and the effective magnetic moments are simply given by eq 3, where the Landè g_J factor is equal to 1.5 for all J levels.

The Stern–Gerlach magnetic analysis allows one to determine the relative population of fine structure levels in the electronic ground state ^3P_J, and an upper limit for the concentration of the metastable ^1D state for the atoms in the supersonic beams, where they are partially relaxed with respect to the conditions of production in the RF plasma.

The analysis of experimental beam transmittances was carried out in two subsequent steps: first we considered as a reasonable hypothesis the exclusive population of the ground ^3P_J state so that, assuming the population of J levels according to a Boltzmann distribution, we get an estimate of the electronic beam temperature T_e from the best fit of beam transmittance data. Experimental results and calculations performed at different electronic temperatures are compared in Fig. 4. We found that, in both He and Ne seeding gases, T_e is lower than the source temperature T_0, but higher than the translational temperature T_f; in addition the Ne seeded beam presents a higher electronic temperature (350 ± 90K) than the He seeded one (90 ± 20K). This is a consequence of both the higher T_0 and T_f reached in the Ne case. The J level populations calculated at T_e are compared in Table 2 with those obtained assuming a Boltzmann distribution at T_0 and T_f, respectively. From an accurate analysis of the data, we can assess that the plasma temperature, T_0, can not be considered an accu-

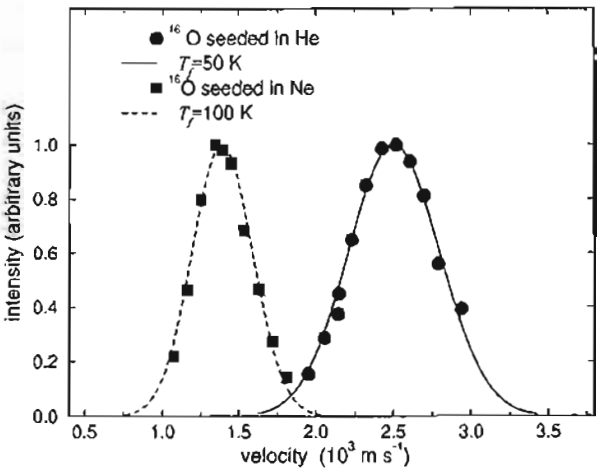

Fig. 3. Measured velocity distributions for the supersonic beams of ^{16}O seeded in He and in Ne. Relevant parameters, as obtained from the best fit of experimental data (solid and dashed curves), are reported in Table 1.

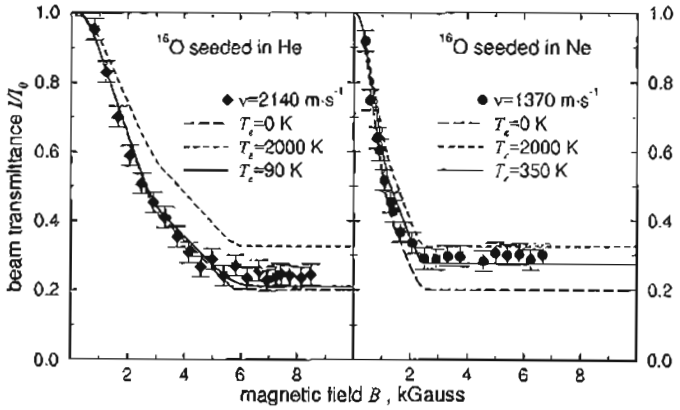

Fig. 4. Beam transmittances of the supersonic beams of ^{16}O seeded in He and in Ne, measured as a function of the magnetic field B at the indicated velocities. Dashed and long-dashed lines are calculated assuming the exclusive population of the ^{3}P state at different, indicated, electronic temperatures T_e; solid lines correspond to best-fit calculations.

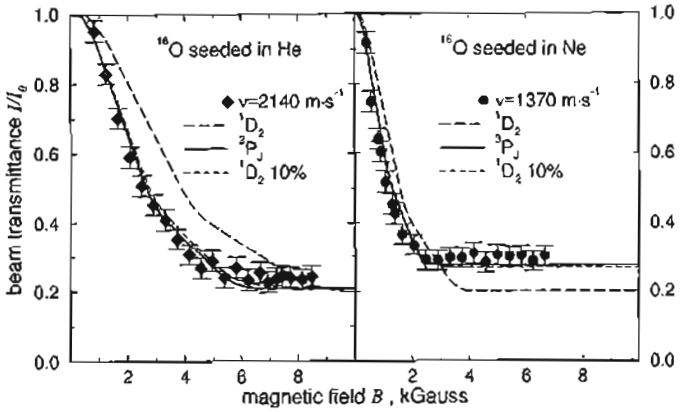

Fig. 5. Beam transmittances of the supersonic beams of ^{16}O seeded in He and in Ne as a function of the magnetic field B. Long-dashed and solid lines are calculated assuming the exclusive presence of ^{1}D or ^{3}P atoms in the beam, respectively; dashed lines are obtained assuming a ^{1}D concentration equal to 10%, which represents an upper limit for its population.

rate parameter for the determination of the J distribution of oxygen atoms in the beam. In particular, in the He seeding case, the relaxation of J = 0 and 1 levels to the ground J = 2 state is almost complete, while in the Ne case it is only partial.

In a second stage we tried to fit the experimental beam transmittances introducing a certain amount of the metastable ^{1}D state, which is present in a small fraction in the beam as was evinced from previous crossed beam experiments on the reactions involving O(^{1}D) as, for instance, the reaction O(^{1}D)+H_2 → OH + H.[2,5,11] Experimental results are compared with calculations carried out using different concentrations for the excited ^{1}D state in Fig. 5. Since the experimental data are not very sensitive to the relative concentration of the metastable state, we can only give an upper limit for the fraction of O atom in the $^1D_2$ state which is ~10% for both Ne and He seeding.

Atomic Nitrogen

Intense supersonic beams of nitrogen atoms have been produced by using the RF discharge source starting from mixtures of N_2 (2.5%) in Ne or He. Figure 6 shows, as an example of the beam velocity analysis, results obtained for the Ne seeding case, while experimental conditions used for beams production and main features of the measured velocity distributions are summarized in Table 1. One of the striking results is the high degree (about 60%) of molecular dissociation achieved in these RF generated atomic beams, which turned out to be critical for performing reactive scattering experiments.

It is well established, since the early work by Foner and Hudson,[55] that electrical discharges in helium-rich N_2/He mixtures produce N atoms not only in the ground electronic $^4S_{3/2}$ state, but also in the excited metastable $^2D_{5/2,3/2}$ and $^2P_{3/2,1/2}$ states in relatively high concentrations. The two electronic excited states lie 2.38 eV [59] and

Table 2. Relative weights W_J of the fine structure levels for O (in the ground electronic $^3P_{2,1,0}$ state) and Cl (in the ground electronic $^2P_{3/2,1/2}$ state) atomic beams calculated assuming Boltzmann distributions at electronic temperatures equal to T_0, T_f (see Table 1), and T_e, respectively (see text)

O atom $^3P_{2,1,0}$ seeded in He			
	$T_e = T_0$	$T_e = T_f$	$T_e = 90 \pm 20$ K
W_2	0.59	0.99	0.94
W_1	0.31	0.01	0.05
W_0	0.10	0.00	0.01
O atom $^3P_{2,1,0}$ seeded in Ne			
	$T_e = T_0$	$T_e = T_f$	$T_e = 350 \pm 90$ K
W_2	0.59	0.93	0.72
W_1	0.31	0.06	0.22
W_0	0.10	0.01	0.06
Cl atom $^2P_{3/2,1/2}$ seeded in He			
	$T_e = T_0$	$T_e = T_f$	$(T_e = 1200 \pm 500$ K)
$W_{3/2}$	0.82	1.00	0.85
$W_{1/2}$	0.18	0.00	0.15
Cl atom $^2P_{3/2,1/2}$ seeded in Ne			
	$T_e = T_0$	$T_e = T_f$	$(T_e = 2200 \pm 700$ K)
$W_{3/2}$	0.79	1.00	0.75
$W_{1/2}$	0.21	0.00	0.25

3.57 eV,[60] respectively, above the ground state. Later experiments,[42,61] which have made use of MW discharge sources, confirmed previous findings on the metastable states formation. The presence of the metastable $^2D_{5/2,3/2}$ and $^2P_{3/2,1/2}$ states in significant concentrations was also recognized in nitrogen beams produced by different techniques[18–22] and used in crossed beam experiments, but the relative populations of N electronic states were not well characterized.

^{14}N atom exhibits both a nuclear **I** ($I = 1$) and electronic **S** spin angular momenta different from zero. In the metastable ^2D and ^2P states the orbital electronic angular momentum **L** is also present. Therefore, both fine (coupling of **L** and **S** to give **J**) and hyperfine interactions (coupling of **J** and **I** to give the total angular momentum **F**) are operative. Two different limiting cases for angular momenta coupling schemes can, in general, be found: in a first coupling scheme, valid when the magnetic field B approaches zero, the quantum number F is the good one; the second scheme is valid in the opposite case, i.e., when B is so large as to decouple **J** from **I** (Back–Goudsmit regime). In this latter limit, the nuclear spin contribution can be neglected, and the effective magnetic moments are exclusively due to **J**. Therefore J is the atomic good quantum number when the magnetic field intensity is in the range

$$\Delta^J_{F\,F+1} < \mu_0 B << \Delta_{J\,J+1}$$

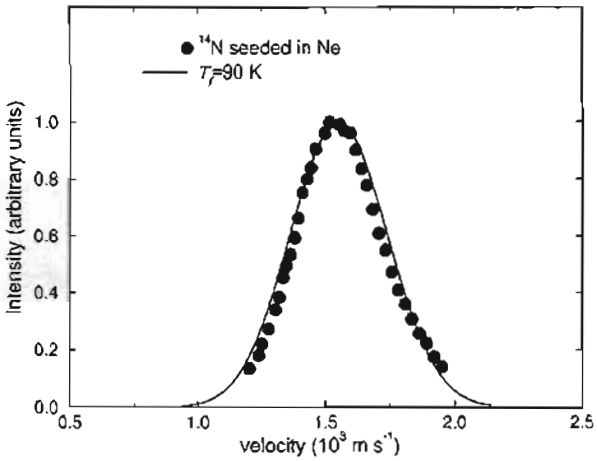

Fig. 6. Measured velocity distribution for the supersonic beam of ^{14}N seeded in Ne. Relevant parameters, as obtained from the best fit of experimental data (solid curve), are reported in Table 1.

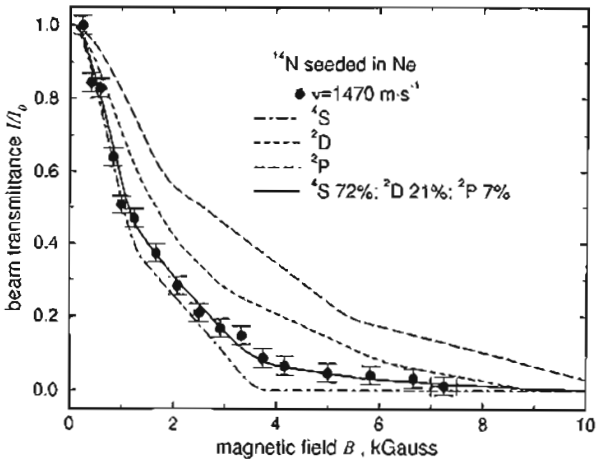

Fig. 7. Beam transmittance for the supersonic beam of ^{14}N seeded in Ne as a function of the magnetic field B at the indicated velocity. Dotted-dashed, dashed, and long-dashed lines are calculated assuming the exclusive population of ^4S, ^2D, and ^2P, respectively; the best-fit calculation is reported as a solid line and corresponds to a total concentration of the two metastable states equal to 28%.

where $\Delta^J_{F\,F+1}$ and $\Delta_{J\,J+1}$ are the hyperfine and fine structure energy separations, respectively. When $\mu_0 B$, which represents the interaction energy of the particle with the magnetic field, is of the order of magnitude of $\Delta_{J\,J+1}$, the Russell–Saunders coupling is broken and the Paschen–Back effect emerges (decoupling of **J** in **L** and **S**). Magnetic field intensities of the present experiments, B ≤ 10 kGauss, are insufficient to produce the Paschen–Back effect in the two metastable nitrogen states as it requires B values higher than 25 kGauss; on the contrary, because of the weak hyperfine coupling constants $\Delta^J_{F\,F+1} \leq 1.6 \cdot 10^{-2}$ cm^{-1},[59–62] a complete Back–

Goudsmit effect is reached even at very low field values ($B \geq 0.1$ kGauss), so that for ^{14}N, good quantum numbers are J and M_J, and effective magnetic moments are given, as for the ^{16}O atom case, by eq 3.

Finally, for the purpose of the magnetic analysis reported below, we consider that fine structure levels of each electronic state are populated according to their multiplicity $2J + 1$, as a consequence of the fact that the fine structure separation is much smaller than the Boltzmann factor kT_e, even if we assume the electronic temperature T_e to be equal to the translational temperatures T_t reported in Table 1.

Beam transmittance results for the Ne seeding case, measured at a velocity $v = 1470$ m · s^{-1} (close to the peak velocity v_{peak}, see Table 1), are presented in Fig. 7 and compared with calculations performed assuming the nitrogen atoms in pure ^4S, ^2D, and ^2P states. Experimental results lie within these calculations, but they are not reproduced by any of the theoretical beam transmittance relative to each pure electronic state. This represents a proof that not only the ground ^4S, but also the excited states are populated in the discharge, and their quenching during beam formation is incomplete. Lin and Kaufmann[61] determined relative populations in the ratios $^4S : ^2D : ^2P = 100 : 4 : 1.3$, while Foner and Hudson[55] found $^4S : ^2D : ^2P = 100 : 17 : 6$, and an even higher total concentration of ^2D and ^2P was determined by Brunetti et al.[42] The concentrations of metastable species obtained in such studies show significant differences as a consequence of the different experimental technique employed (molecular flux or molecular beams), the main consequence being a different quenching effect due to collisions with chamber walls. In addition, various discharge conditions and methods for state analysis were used (spectroscopy and magnetic deflection). Nonetheless, in all previous experiments a constant ratio, equal to 3:1, for the concentrations of N atoms in the ^2D and ^2P states was found. This represents an indication that the two metastable states are produced in a nonstatistical ratio in the plasma, and that their collisional-relaxation processes have almost the same efficiency. On these bases, in the analysis of the present results, we have assumed a $^2D/^2P$ concentration ratio equal to 3 and a fraction c of atoms in the ground ^4S state. Beam transmittance data have then been fitted according to the following expression:

$$\frac{I}{I_0} = c\left(\frac{I}{I_0}\right)_{^4S} + \frac{3(1-c)}{4}\left(\frac{I}{I_0}\right)_{^2D} + \frac{1-c}{4}\left(\frac{I}{I_0}\right)_{^2P} \quad (11)$$

with a best-fit value for c of 0.72 ± 0.04 for both Ne and He seeding gases (see solid line in Fig. 7). The resulting relative population ratios are then $^4S : ^2D : ^2P = 100 : 30 : 10$, and we can attribute the higher concentration of metastable states with respect to previous MW discharge experiments[55,61] to the different experimental conditions used, and in particular, to the RF discharge which operates with a much higher power, and hence, plasma temperature. We note that the considerably high concentration of N(^2D), a form of particularly reactive atomic nitrogen, has made possible the study of reactions which are endoergic for ground state N(^4S), but exoergic for N(^2D), as is the case with molecular hydrogen.[14]

Atomic Chlorine

Supersonic beams of chlorine atoms were generated by using the RF discharge source operating in dilute mixtures of Cl_2 (2.75%) in He and in Ne with a supplementary small fraction of O_2 (~2.75%). By using the RF discharge in 5% Cl_2/He mixtures without O_2 added, the plasma formed is so hot that the nozzle orifice considerably enlarges within a few hours; the presence of small quantities of oxygen significantly reduces the plasma temperature ensuring the stability of the quartz nozzle. The experimental conditions used for supersonic beam production and the main features of the measured velocity distributions are listed in Table 1, and an example of measured velocity distributions, which refers to the Ne seeding case, is reported in Fig. 8. Cl atoms are produced exclusively in their ground ^2P_j state, as the excited ones lie at much higher energies,[58] inaccessible in the RF discharge plasma. The relative population in the beam of the two fine structure levels $J = 3/2$, and 1/2 can be determined via magnetic analysis.

The ^{35}Cl atom in the ground electronic state shows a large fine structure separation ($\Delta_{1/2,3/2} = 109.4$ meV [63,64]) and, because of a nuclear spin quantum number $I = 3/2$, it also possesses a hyperfine structure whose coupling constants are known from the literature.[65,66] As previously observed for the N atom case, magnetic field intensities of the present experiments ($B \leq 10$ kGauss) are insufficient to produce the Paschen–Back effect in the ^2P state of the Cl atom (requiring $B \geq 1.9 \cdot 10^4$ kGauss), while the Back–Goudsmit effect is reached at field values $B \sim 3$ kGauss for the $^2P_{1/2}$ state and ~0.8–0.9 kGauss for the $^2P_{3/2}$ state. We then considered, for the ground $J = 3/2$ fine level, a complete J–I decoupling at all magnetic field intensities used in the experiments, and magnetic moments were calculated according to eq 3. A detailed calculation of Zeeman energies and magnetic moments, according to their definition (eq 4) is instead necessary for the $J = 1/2$ state, since it encompasses a situation of partial nuclear and electronic angular momenta decoupling.

Experimental results for beam transmittances, mea-

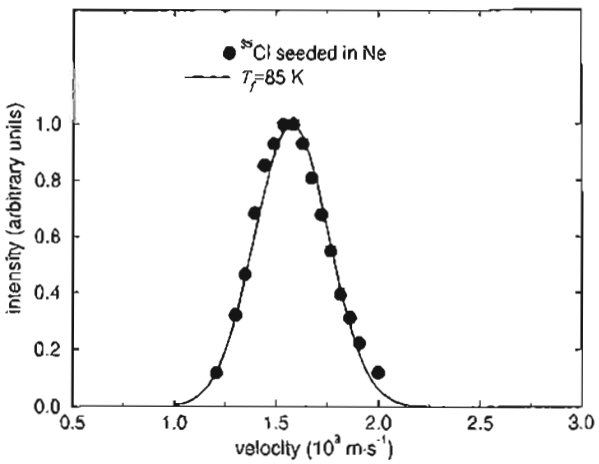

Fig. 8. Measured velocity distribution for the supersonic beam of ^{35}Cl seeded in Ne. Relevant parameters, as obtained from the best fit of experimental data (solid curve), are reported in Table 1.

sured at three different velocities, are reported in Fig. 9 for the Ne seeding case. The analysis of the experimental data was carried out following the lines of ref 45: the magnetic sublevel distribution within each fine structure component is assumed statistical, that is, all hyperfine states within each J level can be considered populated according to their degeneracy because $\Delta^J_{F,F+1} \ll kT$. Therefore, the relative population W_J in the beam of atoms in the fine structure level, J = 1/2, is the only adjustable parameter in the working eq 2, and is directly obtainable from beam transmittance experiments. Lines in Fig. 9 represent calculations performed assuming different relative populations of the excited J = 1/2 state, and the solid line is the calculation with best-fit value of $W_{1/2}$. Results of the present analysis suggest that the $W_{1/2}$ value which gives the best description of the experimental data appears to be slightly dependent on the beam velocity, although the experimental conditions are unable to fully resolve the effect. Specifically, we found $W_{1/2}$ = 0.25 ± 0.03, 0.22 ± 0.03, and 0.20 ± 0.05, respectively at v =1300, 1460, and 1930 m·s^{-1}, with an average value equal to 0.22 ± 0.03. Moreover, for the He seeding case the experimental resolution is even lower because of the higher velocity of the Cl atoms in the beam and of smaller deflections induced by the inhomogeneous field, and only an average $W_{1/2}$ value, equal to 0.15 ± 0.05, has been obtained. These average relative weights W_J are consistent with electronic temperatures T_e equal to 2200 ± 700 and 1200 ± 500 for the Ne and He seeding cases, respectively.

J level populations determined by the present analysis are compared in Table 2 with those obtained assuming a Boltzmann distribution with an electronic temperature T_e equal to T_0 and T_f, respectively. The determined W_J values are found to be close to the populations calculated at T_0 and significantly different from those evaluated at T_f. This comparison suggests that, differently from what was observed in the O atom case, the relaxation of the J = 1/2 level to the ground J = 3/2 state is not very efficient both within the plasma and during the expansion process, and this must be related to the higher value of the energy splitting between the fine structure levels in ^{35}Cl than in ^{16}O.

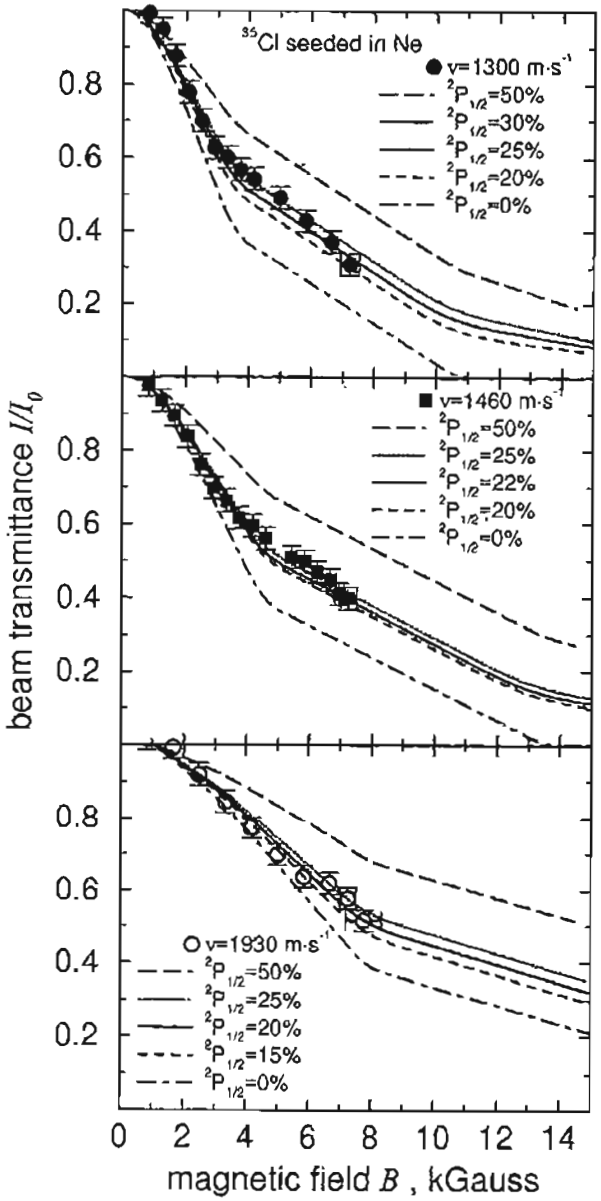

Fig. 9. Beam transmittances for the supersonic beam of ^{35}Cl seeded in Ne, measured as a function of the magnetic field B at three different beam velocities v. Lines are calculated assuming different relative populations $W_{1/2}$ for the $^2P_{1/2}$ state; best-fit calculations are reported as solid lines.

Molecular Beams of O_2 and N_2^*

Magnetic analysis can be applied not only to open shell atoms, but also to paramagnetic states of molecules such as O_2 and N_2, which are present in the plasma because of either incomplete dissociation or atomic recombinations.

Previous studies[48,67] on MW-generated plasma in molecular oxygen at low pressure revealed that O_2 in the effusive beam can populate not only the ground electronic $X\,^3\Sigma_g^-$ state, but also the first excited metastable $a\,^1\Delta_g$ state, which lies ~1 eV over the ground state and has a lifetime of ~44 min.[68] Nitrogen molecules can also be produced in several different long-lived metastable states, formed from atom recombination in the plasma. In particular, previous studies[47] performed with an effusive beam generated from a MW plasma in a He–N_2 mixture, revealed that the excited molecules are essentially in the $A\,^3\Sigma_u^+$ metastable state which has an energy of 6.3 eV and a lifetime of several seconds,[69] and evinced also the presence of a small concentration of the $A'\,^5\Sigma_g^+$ state, lying ~9.8 eV over the ground state, for which an estimate of the mean collision-free lifetime was also given.

Supersonic beams of O_2 molecules were produced by discharging ~100 mbar of 2.5% O_2 in He or Ne mixtures at a nominal RF power of ~300 W. The beam-velocity analysis gave a final translational temperature $T_f \geq 30$ K, corresponding to Mach numbers $M_f \geq 10$; thus the beam has a substantial supersonic character. The situation of angular momenta coupling for $^{16}O_2$ is extremely different in the two examined electronic states. In particular, the ground $^3\Sigma_g^-$ state is very close to a pure Hund's case (b):[70,71] the rotational angular momentum **K** (K = 1, 3, 5, ...) is vectorially coupled to electronic spin **S** (S = 1) to give the total angular momentum **J**, so that each K level splits in three spin-rotational states with quantum number $J = K + 1$, K, and $K-1$. In the presence of a magnetic field insufficient to produce any decoupling effect, as in our experiments, **J** is quantized along the field axis and the resulting quantum number is M_J. Calculation of Zeeman energies and effective magnetic moments associated with each **J** was accomplished by diagonalization of the proper Hamiltonian matrix.[71] The angular momentum coupling scheme for the excited $^1\Delta_g$ state can be described as a pure Hund's case (a): the component Λ ($\Lambda = 2$ in the $^1\Delta_g$ case) of the electronic orbital angular momentum along the molecular axis strongly couples with **K** to give the total angular momentum **J**, from which the first-order effective magnetic moments can be easily calculated.[67] The presence of a certain amount of the first metastable electronic $^1\Delta_g$ state in the beam can be revealed because its paramagnetic character is quite different from that of the ground $^3\Sigma_g^-$ state.

Beam transmittance results for O_2 molecules measured at v = 1210 m·s^{-1} are shown in Fig. 10 together with calculations performed assuming O_2 molecules in pure $^3\Sigma_g^-$ and $^1\Delta_g$ electronic states (dashed and dotted lines). To carry out the beam-transmittance analysis we need to estimate the rotational temperature of the oxygen molecule in the beam, for which only an upper and lower limit can be given: considering that the rotational relaxation in supersonic beams is usually not higher than the translational one, the assumption $T_r \geq T_f = 30$ K holds for the lower limit; for the higher limit, following the consideration that T_r has to be smaller than T_0, and the results of the previously cited experiments with effusive beams, a reasonable value has been estimated to be ~600 K. Beam transmittance data have then been fitted according to the following expression:

$$\frac{I}{I_0} = (1-c)\left(\frac{I}{I_0}\right)_{^3\Sigma_g^-} + c\left(\frac{I}{I_0}\right)_{^1\Delta_g} \qquad (12)$$

where c is the concentration of the $^1\Delta_g$ state, and beam transmittances for the pure states were calculated for the two limiting values of T_r. As a consequence, we determine a lower and upper limit for c equal to 0.15 (when T_r = 600 K, see solid line in Fig. 10) and 0.40 (when T_r = 30 K, see dotted-dashed line in Fig. 10), respectively. These results are in agreement with previous findings on effusive molecular oxygen beams.

Supersonic beams of $^{14}N_2$ molecules have been produced in the RF discharge source (~300 W nominal power) at a total pressure P_0 = 270 mbar, from mixtures of N_2 (2.5%) in Ne or He. The beam velocity analysis gave a final translational temperature $T_f \geq 30$ K, corresponding to $M_f \geq 10$, which gives the beam a substantial supersonic character.

The electronic ground state of nitrogen ($X\,^1\Sigma_g^+$) is diamagnetic but the first excited $A\,^3\Sigma_u^+$ state can be considered to be confined to Hund's case (b) and to have a paramagnetism similar to that of O_2 in the ground $X\,^3\Sigma_g^-$ state; the other possible metastable $A'\,^5\Sigma_g^+$ state is also paramagnetic but no information is available on the Zeeman energies, and, consequently, we have assumed it behaves like a ^{5}S atom of the same mass.

With the experimental device discussed in ref 47, beam-transmittance experiments concerning only the metastable N_2 molecules have been carried out. Data measured at a velocity v = 1470 m·s^{-1} are presented in Fig. 11, together with calculations performed assuming the presence in the beam of a mixture of N_2 molecules in pure electronic $A\,^3\Sigma_u^+$ and $A'\,^5\Sigma_g^+$ states (dashed and dotted lines). Beam-transmittance measurements performed at different velocities v suggest that the $A'\,^5\Sigma_g^+$ concentration increases with beam velocity, as previously observed in the experiments with effusive beams,

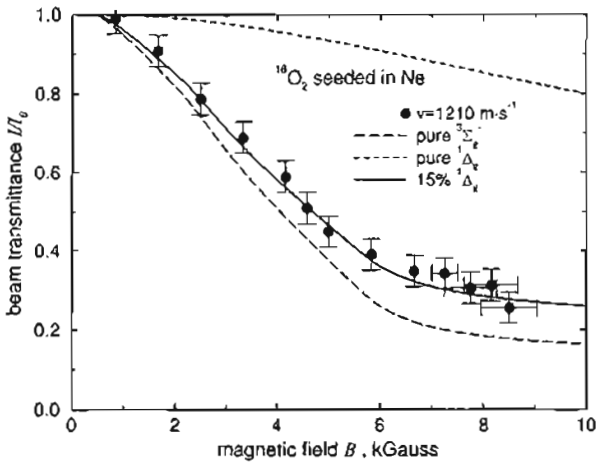

Fig. 10. Beam transmittance I/I_0 of the O_2 beam seeded in Ne, measured as a function of B at $v = 1210$ m·s^{-1}. The long-dashed line is the calculated I/I_0 for a pure $^3\Sigma_g^-$ state, while the dashed line refers to a pure $^1\Delta_g$ state, both calculations being performed assuming a rotational temperature $T_r = 600$ K; solid line is the best-fit calculation which gives the lower limit (~15%) of $^1\Delta_g$ concentration. Similar calculations assuming $T_r = 30$ K give the upper limit ~40%.

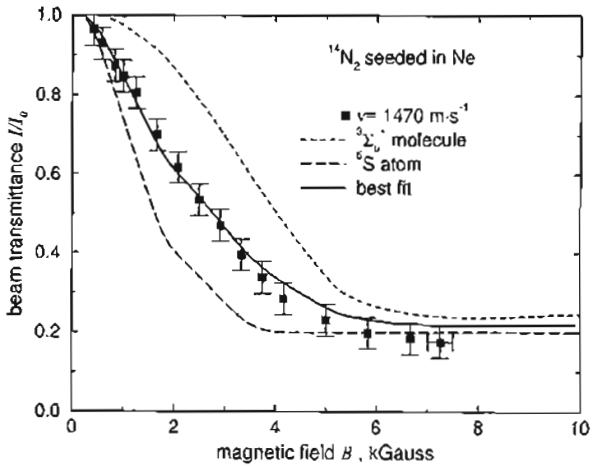

Fig. 11. Beam transmittance I/I_0 of N_2^* beam seeded in Ne, measured as a function of B at $v = 1470$ m·s^{-1}. The dashed and long-dashed lines represent calculated I/I_0 of a beam composed by $A\,^3\Sigma_u^+$ nitrogen molecules (dashed) at a rotational temperature of 300 K and by ^5S atoms of the same mass and velocity (long-dashed); solid line is the best-fit calculation obtained from the one of pure $A\,^3\Sigma_u^+$ molecules introducing a relative concentration equal to 0.55 ± 0.05 of ^5S particles.

and depending on the fact that the mean collision-free lifetime of N_2 molecules in such metastable state is comparable to the time-of-flight in the apparatus.

SUMMARY AND CONCLUSIONS

We produced supersonic beams of O, N, and Cl atoms and of metastable N_2 and O_2 molecules in a high pressure RF discharge beam source and characterized them by coupling velocity selection with magnetic analysis in the transmission mode. We found that oxygen atoms are mainly produced in the electronic ground state ^3P_J and a substantial relaxation within the fine level structure occurs during the beam expansion. In the case of N atoms, not only the ground electronic state ^4S, but also the metastable ^2D and ^2P states are formed in the discharge plasmas; in addition, the relaxation processes are ineffective and atoms in the beams present a high concentration of metastable states. Cl atoms are produced exclusively in the ground electronic ^2P_J state, since excited electronic states are energetically inaccessible at the plasma temperatures. Atoms in the excited fine level $^2P_{1/2}$ are produced in high concentration in the discharge and scarcely relax during the supersonic expansion. Finally, this article shows that an estimate of the relative populations of electronic states in the beam on the basis of plasma temperatures or final translational temperatures can lead to incorrect conclusions.

Acknowledgments. This work was supported by the Italian Consiglio Nazionale delle Ricerche (CNR) and Ministero dell'Università e della Ricerca Scientifica e Tecnologica (MURST), by the European Union through the programs Training and Mobility of Researchers Network "Potential Energy Surfaces for Molecular Spectroscopy and Dynamics" [Contract no. ERB-FMRX-CT96-0088] and the COST D-3 action. Grants from NATO (CRG. 920549) and AFOSR (F617-08-94-C-0013) through EOARD (SPC-94-4042) made possible several aspects of this research.

REFERENCES

(1) (a) Aquilanti, V.; Luzzatti, E.; Pirani, F.; Volpi G.G. *J. Chem. Phys.* **1980**, *73*, 1181. (b) Aquilanti, V; Grossi, G.; Pirani, F. *Electronic and Atomic Collisions, Invited Papers, XIII ICPEAC*; Eichler, J; Hertel, I.V.; Stolterfoht, N., Eds.; North Holland: Amsterdam, 1984; p 441.

(2) Sibener, S.J.; Buss, R.J.; Ng, C.Y.; Lee, Y.T. *Rev. Sci. Instrum.* **1980**, *51*, 167.

(3) Miller, D.R.; Patch, D.F. *Rev. Sci. Instrum.* **1969**, *40*, 1566.

(4) (a) Gorry, P.A.; Grice, R. *J. Phys. E* **1979**, *12*, 857. (b) Hoffman, S.M.A.; Smith, D.J.; Grice, R. *Mol. Phys.* **1983**, *49*, 621. (c) Steele, T.A.; Bradshaw, N.; Grice, R. *Mol. Phys.* **1985**, *56*, 1117.

(5) Buss, R.J.; Casavecchia, P.; Hirooka, T.; Sibener, S.J.; Lee, Y.T. *Chem. Phys. Lett.* **1981**, *82*, 386.

(6) (a) Balucani, N.; Beneventi, L.; Casavecchia, P.; Volpi, G.G. *Chem. Phys. Lett.* **1991**, *180*, 34. (b) Balucani, N.;

Beneventi, L.; Casavecchia, P.; Volpi, G.G.; Kruus, E.J.; Sloan, J.J. *Can. J. Chem.* **1994**, *72*, 888. (c) Alagia, M.; Balucani, N.; Casavecchia, P.; Volpi, G.G. *J. Phys. Chem. A* **1997**, *101*, 6455.

(7) (a) Balucani, N.; Beneventi, L.; Casavecchia, P.; Stranges, D.; Volpi, G.G. *J. Chem. Phys.* **1991**, *94*, 8611. (b) Balucani, N.; Casavecchia, P.; Stranges, D.; Volpi, G.G. *Chem. Phys. Lett.* **1993**, *211*, 469. (c) Balucani, N.; Casavecchia, P.; Stranges, D.; Volpi, G.G. In preparation.

(8) (a) Casavecchia P., Balucani, N., and Volpi, G.G. In *Research in Chemical Kinetics*; Compton, R.G.; Hancock, G., Eds.; Elsevier: Amsterdam, 1993; Vol. 1, p 1. (b) Casavecchia P., Balucani, N., and Volpi, G.G. In *Advanced Series in Chemical Physics*. Vol. 6, *The Chemical Dynamics and Kinetics of Small Radicals;* Wagner, A.; Liu, K., Eds.; World Scientific: Singapore, 1995, p 365.

(9) Alagia, M.; Balucani, N.; Casavecchia, P.; Stranges, D.; Volpi, G.G. *J. Chem. Soc., Faraday Trans.* **1995**, *91*, 575.

(10) Alagia, M.; Balucani, N.; Casavecchia, P.; Laganà, A.; Ochoa de Aspuru, G.; van Kleef, E.H.; Volpi, G.G.; Lendvay, G. *Chem. Phys. Lett.* **1996**, *258*, 323.

(11) Alagia, M.; Balucani, N.; Cartechini, L.; Casavecchia, P.; van Kleef, E.H.; Volpi, G.G.; Kuntz, P.J.; Sloan, J.J. *J. Chem. Phys.* Submitted.

(12) (a) Alagia, M.; Balucani, N.; Casavecchia, P.; Stranges, D.; Volpi, G.G. *J. Chem. Phys.* **1993**, *98*, 2459. (b) ibid., 8341. (c) Alagia, M.; Balucani, N.; Casavecchia, P.; Stranges, D.; Volpi, G.G.; Clary, D.C.; Kliesch, A.; Werner, H.-J. *Chem. Phys.* **1996**, *207*, 389.

(13) Alagia, M.; Balucani, N.; Cartechini, L.; Casavecchia, P.; Van Kleef, E.H.; Volpi, G.G.; Aoiz, F.J.; Bañares, L.; Schwenke, D.W.; Allison, T.C.; Mielke, S.L.; Truhlar, D.G. *Science* **1996**, *273*, 1519.

(14) Alagia, M.; Balucani, N.; Cartechini, L.; Casavecchia, P.; Volpi, G.G. In preparation.

(15) Alagia, M.; Balucani, N.; Cartechini, L.; Casavecchia, P.; van Kleef, E.H.; Volpi, G.G. In preparation.

(16) Valentini, J.J.; Coggiola, M.J.; Lee, Y.T. *Rev. Sci. Instrum.* **1977**, *48*, 58.

(17) Zhang, J.; Lee, Y.T. *J. Phys. Chem.* A **1997**, *101*, 6485.

(18) Love, R.L.; Herrmann, J.M.; Bickes, R.W.Jr.; Bernstein, R.B. *J. Am. Chem. Soc.* **1977**, *99*, 8316.

(19) Bickes, R.W.Jr.; Newton, K.R.; Herrmann, J.M.; Bernstein, R.B. *J. Chem. Phys.* **1976**, *64*, 3648.

(20) Ringer, G.; Gentry, W.R. *J. Chem. Phys.* **1979**, *71*, 1902.

(21) Porter, R.A.R.; Brown, G.R.; Grosser, A.E. *Chem. Phys. Lett.* **1979**, *61*, 313.

(22) Pollard, J.E. *Rev. Sci. Instrum.* **1992**, *63*, 1771.

(23) Reuss, J. *In Atomic and Molecular Beams Methods*; Scoles G., Ed.; Oxford University Press: New York, 1987, and references therein.

(24) Meschi, D.J.; Searcy, A.W. *J. Chem. Phys.* **1969**, *51* 5134.

(25) Pritchard, D.E.; Carter, G.M.; Chu, F.Y.; Kleppner, D. *Phys. Rev. A* **1970**, *2*, 1922.

(26) Michael, E.G.; Sides, G.D.; Tang, S.Y.; Muschlitz, E.E.Jr. *J. Appl. Phys.* **1973**, *44*, 5356.

(27) Amirav, A.; Even, U.; Jortner, J.; Kleinman, L. *J. Chem. Phys.* **1980**, *73*, 4217.

(28) Anderle, M.; Bassi, D.; Iannotta, S.; Marchetti, S.; Scoles, G. *Phys. Rev. A* **198**, *23*, 34.

(29) Amirav, A.; Navon, G. *Chem. Phys.* **1983**, *82*, 253.

(30) Mettes, J.; Heijmen, B.; Reuss, J.; Lainé, D.C. *Chem. Phys.* **1984**, *87*, 1.

(31) Cox, D.M.; Trevor, D.J.; Whetten, R.L.; Rohlfing, E.A.; Kaldor, A. *J. Chem. Phys.* **1986**, *84*, 4651, and references therein.

(32) Weiser, C.; Siska, P.A. *Rev. Sci. Instr.* **1987**, *58*, 2124; *Z. Phys. D* **1988**, *10*, 165.

(33) (a) Kuebler, N.A.; Robin, M.B.; Yang, J.J.; Gedanken, A.; Herrick, D.R. *Phys. Rev. A* **1988**, *38*, 737. (b) Gedanken, A.; Kuebler, N.A.; Robin, M.B.; Herrick, D.R. *J. Chem. Phys.* **1989**, *90*, 3981. (c) Gedanken, A.; Kuebler, N.A.; Robin, M.B.; Herrick, D.R. *J. Am. Chem. Soc.* **1989**, *111*, 5568.

(34) Berkling, K.; Schlier, Ch.; Toschek, P. *Z. Phys.* **1962**, *168*, 81.

(35) (a) Hishinuma, N.; Sueoka, O. *Chem. Phys. Lett.* **1983**, *98*, 414. (b) Hishinuma, N.; Sueoka, O. *Chem. Phys. Lett.* **1985**, *121*, 293.

(36) Rothe, E.W.; Neynaber, R.H.; Trujillo, S.M. *J. Chem. Phys.* **1965**, *42*, 3310.

(37) Stolte, S. In *Atomic and Molecular Beams Methods*; Scoles G., Ed.; Oxford University Press: New York, 1987, and references therein.

(38) Zandee, L.; Reuss, J. *Chem. Phys.* **1977**, *26*, 327.

(39) Parrish, D.D.; Herm, R. *J. Chem. Phys.* **1971**, *54*, 327.

(40) Struve, W.S.; Krenos, J.R.; McFadden, D.L.; Herschbach, D.R. *J. Chem. Phys.* **1975**, *62*, 404.

(41) Shi, X.; Herschbach, D.R.; Worsnop, D.R.; Kolb, C.E. *J. Phys. Chem.* **1993**, *97*, 2113.

(42) Brunetti, B.; Liuti, G.; Pirani, F.; Luzzatti, E. *Chem. Phys. Lett.* **1981**, *84*, 201.

(43) Aquilanti, V.; Candori, R.; Pirani, F. *J. Chem. Phys.* **1988**, *89*, 6157.

(44) (a) Aquilanti, V.; Luzzatti, E.; Pirani, F.; Volpi, G.G. *J. Chem. Phys.* **1988**, *89*, 6165. (b) Aquilanti, V.; Candori, R.; Cappelletti, D.; Luzzatti, E.; Pirani, F. *Chem. Phys.* **1990**, *145*, 293.

(45) Aquilanti, V.; Candori, R.; Cappelletti, D.; Lorent, V. Pirani, F. *Chem. Phys. Lett.* **1992**, *192*, 145.

(46) (a) Aquilanti, V.; Candori, R.; Mariani, L.; Pirani, F.; Liuti, G. *J. Phys. Chem.* **1989**, *93*, 130. (b) Aquilanti, V.; Cappelletti, D.; Lorent, V.; Luzzatti, E. Pirani, F. *Chem. Phys. Lett.* **1992**, *192*, 153. (c) Aquilanti, V.; Cappelletti, D.; Lorent, V.; Pirani, F. *J. Phys. Chem.* **1993**, *97*, 2063. (d) Aquilanti, V.; Cappelletti, D.; Pirani, F. *J. Chem. Soc., Faraday Trans.* **1993**, *89*, 1467.

(47) Cappelletti, D.; Liuti, G.; Luzzatti, E.; Pirani, F. *J. Chem. Phys.* **1994**, *101*, 1225.

(48) (a) Aquilanti, V.; Ascenzi, D.; Cappelletti, D.; Pirani, F. *Int. J. Mass Spectrom. Ion Processing* **1995**, *149/150*, 355. (b) Aquilanti, V.; Ascenzi, D.; Cappelletti, D.; Pirani, F. *J. Chin. Chem. Soc.* **1995**, *42*, 263.
(49) (a) Aquilanti, V.; Ascenzi, D.; Cappelletti, D.; Pirani, F. *Nature* **1994**, *371*, 399. (b) Aquilanti, V.; Ascenzi, D.; Cappelletti, D.; Pirani, F. *J. Phys. Chem.* **1995**, *99*, 13620.
(50) Ramsey, N.F. *Molecular Beams*; Clarendon Press: Oxford, 1969.
(51) (a) Anderson, J.B.; Andres, R.P.; Fenn, J.B. *Adv. Chem. Phys.* **1966**, *3*, 275. (b) Miller, D.R. In *Atomic and Molecular Beams Methods*; Scoles G., Ed.; Oxford University Press: New York, 1987, and references therein.
(52) Arnold, S.J.; Rojeska H. *Appl. Opt.* **1973**, *12*, 169.
(53) Fite, W.L.; Brackman, R.T. *Phys. Rev.* **1959**, *113*, 815.
(54) Rapp, D.; Englander-Golden, P.; Broglia, D.D. *J. Chem. Phys.* **1965**, *42*, 4081.
(55) Foner, S.N.; R.L. Hudson, R.L. *J. Chem. Phys.* **1962**, *37*, 1662.
(56) Mark, T.D. *J. Chem. Phys.* **1975**, *63*, 3731.
(57) Brook, E.; Harrison, M.F.A.; Smith, A.C.H. *J. Phys. B* **1978**, *11*, 3115.
(58) Moore. C.E. *Atomic Energy Levels*, National Bureau of Standards: Washington, DC, 1949; Vol. 1.
(59) Radford, H.E.; Evenson, K.M. *Phys. Rev.* **1967**, *168*, 70.
(60) McConkey, J.W.; Herman, L. *Phys. Lett.* **1964**, *12*, 13.
(61) Lin, C.L.; Kaufmann, F. *J. Chem. Phys.* **1971**, *55*, 3760.
(62) Heald, M.A.; Besinger, K. *Phys. Rev.* **1954**, *96*, 645.
(63) Davis, L.Jr.; Feld, B.T.; Zabel, C.W.; Zacharias, J.R. *Phys. Rev.* **1949**, *76*, 1076.
(64) Dagenais, M.; Johns, J.W.C.; McKellar, A.R.W. *Can. J. Phys.* **1976**, *54*, 1438.
(65) Jaccarino, V.; King, J.G. *Phys. Rev.* **1951**, *83*, 471.
(66) Jaccarino, V.; King, J.G. *Phys. Rev.* **1951**, *84*, 852.
(67) (a) Falick, A.M.; Mahan, B.H.; Myers, R.J. *J. Chem. Phys.* **1964**, *42*, 1837. (b) Arrington, C.A.Jr.; Falick, A.M.; Myers, R.J. *J. Chem. Phys.* **1971**, *55*, 909.
(68) (a) Kolts, J.H.; Setser, D.W. In *Reactive Intermediates in the Gas Phase—Generation and Monitoring*; Setser, D.W., Ed.; Academic Press: New York, 1976. (b) Badger, R.M.; Wright, A.C.; Whitlock, R.F. *J. Chem. Phys.* **1965**, *43*, 4345.
(69) Radzig, A.A.; Smirnov, B.M. *Reference Data on Atoms, Molecules and Ions*; Springer-Verlag: Berlin, 1985.
(70) Herzberg, G. *Molecular Spectra and Molecular Structure*. Vol. 1, *Spectra of Diatomic Molecules*. Van Nostrand: Princeton, NJ, 1967.
(71) Tinkham, M.; Strandberg, M.W.P. *Phys. Rev.* **1955**, *97*, 937 and 951.